Superconductivity in the surface layer of $SrTiO_3/(Ba_{0.9}Nd_{0.1})CuO_{2+x}/CaCuO_2$ heteroepitaxial structures

G. Balestrino, S. Lavanga, P. G. Medaglia, P. Orgiani, and A. Tebano
INFM - Università di Roma "Tor Vergata" Dipartimento di Ingegneria Meccanica, Via del Politecnico 1, 00133 Roma, Italy
(Received 21 December 2001; revised manuscript received 8 April 2002; published 5 September 2002)

We report on the pulsed laser deposition and characterization of the $(BaCuO_2)_m/(CaCuO_2)_n$ heterostructures deposited on to $SrTiO_3$ (001) substrates. For some of the heterostructures realized it was possible to find a high temperature superconducting transition. These thin films represent one of the simplest structures containing the two structural subunits constituting all the existing high temperature cuprate superconductors. We studied the superconducting properties of these thin films with m varying between 2 and 5 and n varying between 0.66 and 6. We discuss the results also in comparison with those obtained for the superconducting $BaCuO_2/CaCuO_2$ superlattices. The results obtained can offer new possibilities to study the fundamental physical mechanism of high temperature superconductivity.

DOI: 10.1103/PhysRevB.66.094505 PACS number(s): 74.76.Bz, 74.80.Dm, 81.15.Fg

Atomic layer by atomic layer deposition techniques applied to oxide compounds have opened perspectives for the engineering of thin films of interesting materials and complex heterostructures with improved functional properties.[1,2] The same approach has been used to investigate fundamental properties of high temperature superconducting (HTS) materials.[3–10] In this case the goal was to unravel the key features of high T_c superconductivity reducing the intrinsically high degree of structural complexity typical of HTS compounds grown under thermodynamic equilibrium conditions. Such an approach is based on the simple observation that all existing HTS cuprates exhibit a layered structure, with a stacking sequence of two structural subunits having different functions, namely the charge reservoir (CR) block and the infinite layer (IL) superconducting block.[11] The IL block always consists of CuO_2 planes separated by an alkaline earth (mostly Ca) plane. While the structure and the chemical composition of the CR block vary from compound to compound. It is commonly accepted that excess charge carriers (usually holes) are transferred from the CR block to the IL block thus giving rise to superconductivity in the otherwise insulating CuO_2 planes. On the basis of this simple model, several authors have tried to synthesize artificial HTS structures.[12,13] Relevant results were obtained in the case of $(BaCuO_{2+x})_m/(CaCuO_2)_n$ superconducting artificial structures where $(BaCuO_{2+x})_m$ and $(CaCuO_2)_n$ play the role of the CR and the IL blocks, respectively.[14] Such artificial HTS materials were successively used to investigate the influence of some relevant structural features on the superconducting properties. Following this approach, the thickness of the individual constituent blocks was varied in a wide range, well beyond the possibility offered by conventional HTS materials. For instance, high crystallographic quality $2\times n$ superlattices (n is the number of $CaCuO_2$ unit cells in the IL block) were grown with n varying from 1 to 15.[15] Among them, the 2×2 superlattices proved to be optimally doped and showed the highest superconducting transition temperature with T_c (zero resistance temperature) above 80 K. For thicker IL blocks the critical temperature decreases until, finally, for $n\geqslant 11$, the artificial structure is no longer superconducting. Such an effect was explained by considering the decrease of the effective carrier concentration per CuO_2 plane in thick IL blocks. This result showed that carriers, holes injected from the CR block, do not localize at the interfaces, but rather distribute homogeneously over the whole IL block. Successively, artificial $(BaCuO_{2+x})_m/(CaCuO_2)_2$ structures were synthesized to investigate the interlayer coupling between adjacent superconducting $CaCuO_2$ blocks.[16] In this case the thickness of the CR block was gradually increased up to $m=10$. It was found that interlayer coupling is not essential for high-T_c superconductivity: giant CR blocks, thicker than 20 Å ($n\geqslant 5$), depress T_c only slightly while they increase the two-dimensions character of the superconductivity.[17] Such results confirmed those previously obtained from ultrathin films of conventional materials.[18,19]

More recently a thin film of the $CaCuO_2$ IL compound, capped with an insulating layer of Al_2O_3, was used to produce a field-effect device. Field-effect doping was induced by an electric field applied to a Pt gate deposited on the Al_2O_3 layer. At high hole and electron doping levels, superconductivity was induced in the otherwise insulating $CaCuO_2$ layer.[20] This approach allowed the investigation of the superconducting phase diagram of $CaCuO_2$ both on the n and p doping sides. For p doping a maximum T_c of 89 K was found, in good agreement with the results reported in Ref. 7 for external doping. Field-effect doping offers an important advantage relative to the external doping by a CR block: it gives the possibility of studying the physical properties of HTS cuprates as a function of doping on the same sample varying a single external parameter, namely, the applied gate voltage. However, in this approach, the effective thickness of the superconducting IL block is not clearly identified, moreover the presence of a cap layer, necessary for the field-effect doping, can prevent the use of important surface probes such as angle resolved photoemission or *in situ* tunnel spectroscopy.

In this paper we show that high-T_c superconductivity can be achieved in ultrathin $CaCuO_2$ layers at the surface of $SrTiO_3/BaCuO_{2+x}/CaCuO_2$ heteroepitaxial structures. In this case $CaCuO_2$ doping is obtained by charge transfer from

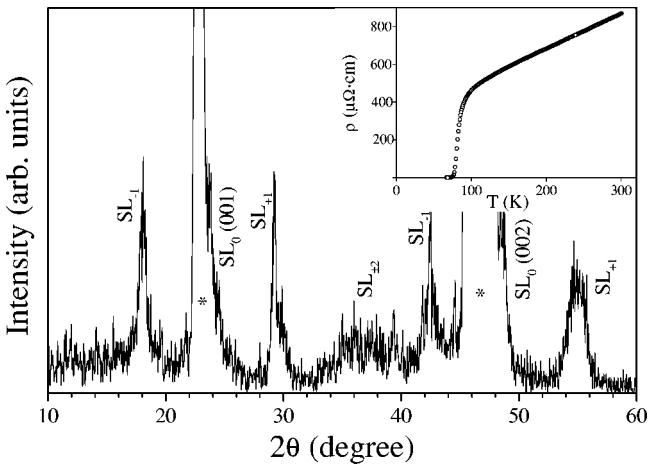

FIG. 1. $\theta-2\theta$ XRD spectrum of a 2×2 superlattice film grown on a (001) $SrTiO_3$ substrate(*). In the inset the corresponding resistivity measurement is shown.

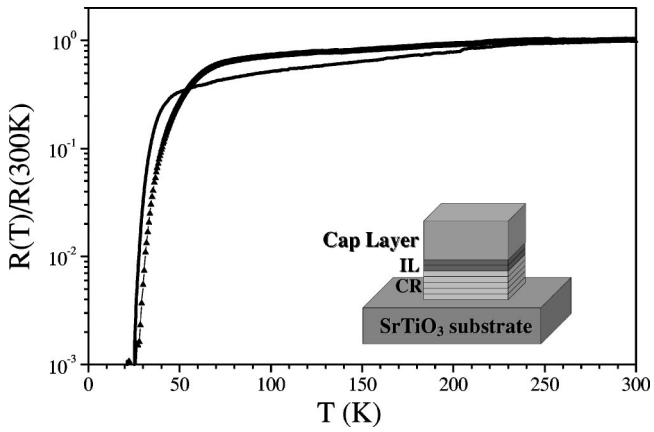

FIG. 2. Resistance (normalized to the 300-K value) behavior of the $[Ba_{0.9}Nd_{0.1}CuO_{2+x}]_m/[CaCuO_2]_2$ artificial structure with $m=2$ (full line) and 5 (triangle). In the inset the m/n structure is roughly sketched.

the underlaying $BaCuO_{2+x}$ CR block. The effective doping can be varied by varying the thickness of the $CaCuO_2$ overlayer. The approach proposed in the present paper offers important perspectives both for the investigation of high-T_c superconductivity by surface techniques and for the research of high T_c superconductivity in other insulating related systems externally doped by a $BaCuO_{2+x}$ underlying layer.

All samples utilized for the present work were grown on $SrTiO_3(001)$ substrates by pulsed laser deposition. All the films were grown starting from $(Ba_{0.9}Nd_{0.1})CuO_2$ and $CaCuO_2$ ceramic targets. The growth temperature was about 640 °C and the molecular oxygen pressure was ≈1 mbar. Further details on the growth procedure was given in Ref. 21. At the end of the deposition procedure an amorphous protecting layer of electrically insulating $CaCuO_2$ was deposited on the top of the film at temperatures lower than 100 °C to prevent sample degradation in air. Electrical transport measurements were carried out by standard four-probe dc technique. A tiny amount of Nd was added to the CR block to increase its thermodynamic stability.[16] In order to realize such epitaxial heterostructures, layer-by-layer growth of the constituent $BaCuO_2$ and $CaCuO_2$ layers must be achieved. *In situ* reflection high-energy electron diffraction (RHEED) at relatively low pressure ($P_{O_2}\approx10^{-4}$ mbar) has shown that the growth mechanism is two dimensional.[22] *Ex situ* x-ray diffraction (XRD) analysis confirmed such findings. Unfortunately, at the high oxygen pressure (about 1 mbar) needed to dope the Ba-based block, RHEED cannot be used. However, even in such a case, the thickness of each layer can be carefully calibrated, *a posteriori*, by XRD spectra.[23,24] Because well defined XRD spectra cannot be obtained from such a structure made of few atomic planes, we decided to calibrate the growth rate of the CR and IL block growing a relatively thick $[((Ba_{0.9}Nd_{0.1})CuO_{2+x})_2/(CaCuO_2)_2]_{25}$ superlattice prior to the deposition of each heterostructure. A typical XRD spectrum of the $[((Ba_{0.9}Nd_{0.1})CuO_{2+x})_2/(CaCuO_2)_2]_{25}$ superlattice, with $T_c\simeq80$ K, is shown in Fig. 1. From the angular distance between the first order satellite peaks (SL_{-1} and SL_{+1}) it is possible to obtain the period Λ of the superlattice, $\Lambda=\lambda/(\sin\theta_{+1}-\sin\theta_{-1})$, where θ_{+1} and θ_{-1} represent the angular positions of the first order satellite peaks and λ represents the x-ray wavelength. The average lattice parameter $\bar{c}$ can be estimated from the angular positions of the zeroth order SL_0 $(00l)$ peak, θ_0, $\bar{c}=l\lambda/2\sin\theta_0$. The presence of sharp superlattice peaks allows a precise *a posteriori* calibration of the growth rate of the two constituent layers (see Ref. 25). Once growth rates have been calibrated, the number of laser shots on each target is adjusted to obtain the aimed $SrTiO_3/((Ba_{0.9}Nd_{0.1})CuO_{2+x})_m/(CaCuO_2)_n$ heterostructure. $SrTiO_3/((Ba_{0.9}Nd_{0.1})CuO_{2+x})_m/(CaCuO_2)_n$ heterostructures, with $m=2$ and 5, were deposited (simply stopping the deposition after one sequence). No relevant differences in the transition temperature were found (Fig. 2). The slight difference in the transition width can be possibly ascribed to small difference in the samples homogeneities. This result shows that external doping of the $CaCuO_2$ layer does not depend strongly on the thickness of the CR block at least for $m\geqslant2$. Successively m was kept equal to 5 and n was varied from 0.66 to 6. In the case of $n=0.66$, the number of laser shots on the $CaCuO_2$ target was 2/3 of those required to complete a single unit cell $CaCuO_2$ layer. In Fig. 3 we show the behavior of resistance versus temperature for different values of n. Several interesting features can be recognized.

(i) T_c varies with n. The maximum value, about 30 K, is obtained for $n=2$, for $n\geqslant5$, and for $n<1$ the heterostructure becomes nonsuperconducting.

(ii) The slope of the curve R versus T is always positive (''metallic'' behavior) except for heterostructures having $n\geqslant5$. In the case of the $n=0.66$ sample the slope is positive above 100 K but becomes negative at low temperatures.

The critical temperature of such ultrathin structures was also inductively measured by a mutual inductance method. In our measurement technique, a single coil is pressed against the superconducting film and another one is pressed on the back side of the substrate. Coil and film surfaces are separated by a thin insulating mica foil (about 200 μm thick).

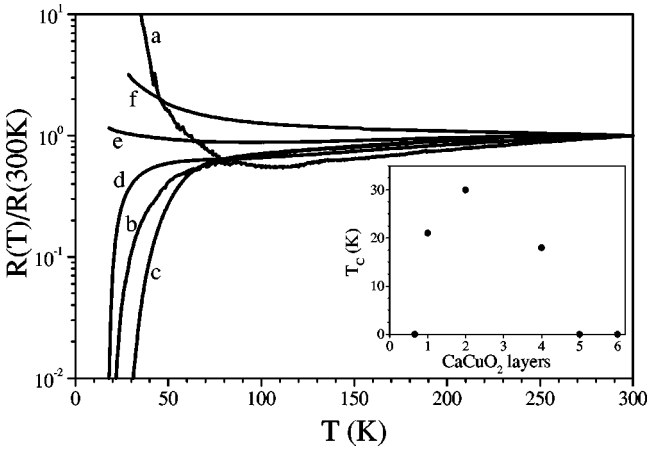

FIG. 3. Resistance (normalized to the 300-K value) behaviour of $[Ba_{0.9}Nd_{0.1}CuO_{2+x}]_5/[CaCuO_2]_n$ artificial structures: (a) $n=0.66$, (b) $n=1$, (c) $n=2$, (d) $n=4$, (e) $n=5$, and (f) $n=6$. In the inset the critical temperature (zero resistance point) vs the number of $CaCuO_2$ IL layers is shown.

The coil is driven by an audio frequency sine-wave current ($f_o=1$ KHz) generated by a lock-in amplifier. The first harmonic signal U_{11} (at the same frequency of the driving signal f_o) on the pick-up coil is monitored as a function of the temperature. A very small driving current flowing in the coil (I_{coil}) gives rise to a magnetic field in proximity to the film surface. In the superconducting state, a sine-wave shielding current is induced in the film. Such a diamagnetic behavior results in a decrease of the pick-up coil signal. In Fig. 4 the behavior of the first harmonic signal versus temperature is reported for a 5/2 structure. The T_c of the 5/2 structure (usually the temperature where the 2^{nd} derivative of magnetization is zero) is about 35 K with a large transition width (larger than 15 K). The full sample becomes superconductive at temperature below about 10 K.

In $BaCuO_2/CaCuO_2$ superlattices each IL block is sandwiched between two structurally coherent $BaCuO_2$ layers. The presence of an incoherent interface between the IL layer and the protecting cap layer could lead to the suppression of

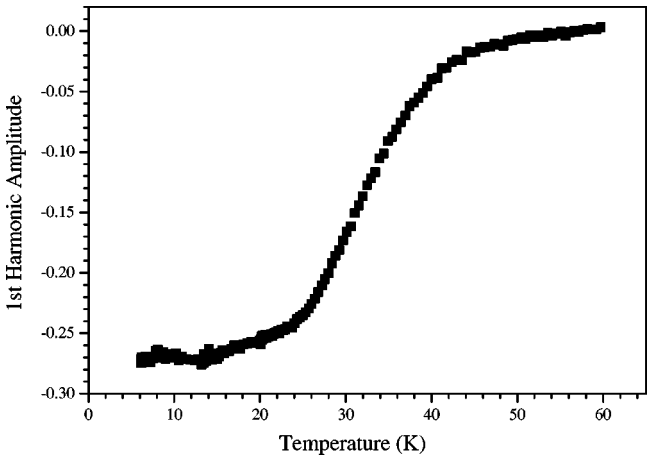

FIG. 4. Meissner transition inductively measured for a 5/2 structure.

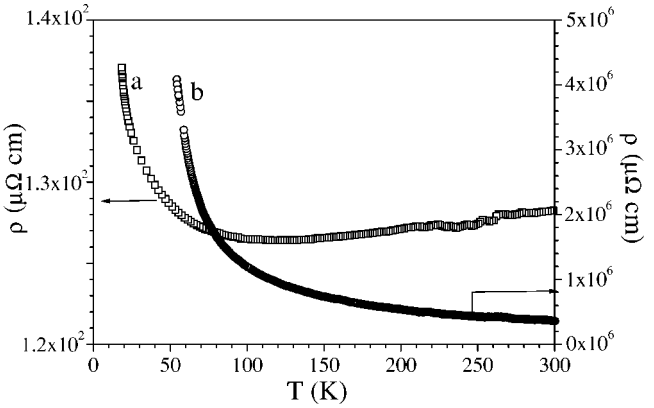

FIG. 5. Resistivity measurements of (a) $Ba_{0.9}Nd_{0.1}CuO_{2+x}$ and (b) $CaCuO_2$ parent compounds.

superconductivity. The T_c dependence on n can be explained considering the variation of the effective charge carrier concentration per CuO_2 plane. That is, all bilayers are grown in the same conditions of temperature and oxygen pressure, therefore we expect the same content of extra oxygen ions in the CR block. In Ref. 15, it was shown that extra charge carriers from the CR block distribute homogeneously over the IL block. If the thickness of the IL block exceeds a critical value, the effective carrier concentration becomes lower than the minimum value for superconductivity (about 0.05 holes per CuO_2 unit) and the superlattice becomes nonsuperconducting. The same mechanism holds here. Furthermore, even if the ill defined contact geometry does not allow a precise measurement of the sheet resistance ($R_\square$), we could estimate a value of 10–20 KΩ for the 5/5 structure (curve *e* in Fig. 3) which marks the superconductor-to-insulator (SI) transition. Such $R_\square$ value is not far from the threshold value reported in Refs. 26 and 27, even if in the present case the SI transition is driven by the carrier concentration rather than the film thickness. We also notice that in Ref. 15 the critical value of n was found to be ≈ 11, roughly twice the value found in the present work. Such an effect could be expected if we consider that, in the case of the bilayers, doping occurs from one side only, while in the case of superlattices, the IL block is sandwiched between two CR blocks. For $n<2$, the T_c decreases again and the sample becomes non superconducting for $n<1$. Such behavior is a consequence of both the overdoping of the IL block and of the increased role of disorder at the interface between the IL and the CR block. For $n<1$, no percolative path can be found in the $CaCuO_2$ overlayer and the R versus T behavior essentially depends on the $(Ba_{0.9}Nd_{0.1})CuO_{2+x}$ layer. Finally the behavior of the normal state resistivity for our heterostructures can be understood considering data reported in Fig. 5. In Fig. 5 we report the R versus T behavior for a pure $CaCuO_2$ and $(Ba_{0.9}Nd_{0.1})CuO_{2+x}$ film. Resistivity of the pure $CaCuO_2$ film is much higher relative to that of the $(Ba_{0.9}Nd_{0.1})CuO_{2+x}$ film and increases continuously when temperature decreases. This result is expected because the $CaCuO_2$ film is well charge compensated. Conversely, the $(Ba_{0.9}Nd_{0.1})CuO_{2+x}$ film, where an excess of carriers (holes)

exists due to the extra oxygen ions, shows a much lower resistivity with an almost metallic behavior except that at low temperature. As expected, neither of the two compounds shows any trace of superconductivity. In the case of the $SrTiO_3/((Ba_{0.9}Nd_{0.1})CuO_{2+x})_5/(CaCuO_2)_n$ artificial structures, when the doping level is high enough, the electrical transport properties are determined by the $CaCuO_2$ layer: the behavior of resistance versus temperature is metallic and, at low temperature, a superconducting transition occurs. Underdoped $CaCuO_2$ layers show a behavior which has a strong resemblance to that of the pure undoped $CaCuO_2$ compound. On the other hand, when the thickness of the $CaCuO_2$ overlayer becomes smaller than one unit cell the behavior resembles, as expected, that of the underlying $((Ba_{0.9}Nd_{0.1})CuO_{2+x})$ pure compound, namely metallic at high temperature and ''semiconducting'' below about 100 K.

The occurrence of superconductivity in the top layer of a $SrTiO_3/((Ba_{0.9}Nd_{0.1})CuO_{2+x})_5/(CaCuO_2)_n$ artificial structures demonstrates that charge injection in a IL cuprate structure is the essential feature for high- T_c superconductivity. Furthermore we have shown that the doping level of the overlayer can be varied in a wide range changing the number of $CaCuO_2$ unit cells. *Ex situ* electrical transport measurements still require an amorphous protective cap layer, about 50 Å thick, to prevent fast degradation of the surface layer. However, it is easy to foresee that *in situ* surface measurements applied to the controlled surfaces of these artificial structures could be very useful to elucidate the complex physics of the high temperature superconducting cuprates.

[1] M. Kanai, T. Kawai, and S. Kawai, Appl. Phys. Lett. **58**, 771 (1991).

[2] Q. Li, X.X. Xi, X.D. Wu, A. Inam, S. Vadlamannati, W.L. McLean, T. Venkatesan, R. Ramesh, D.W. Hwang, J.A. Martinez, and L. Nazar, Phys. Rev. Lett. **64**, 3086 (1990).

[3] W.K. Park and Z.G. Khim, Phys. Rev. B **61**, 1530 (2000).

[4] S. Berger, D.G. Crété, J.P. Contour, K. Bouzehouane, J.L. Maurice, and O. Durand, Phys. Rev. B **63**, 144506 (2001).

[5] D. Budelmann, S. Ostertun, M. Rubhausen, A. Bock, M. Schilling, H. Burkhardt, U. Merkt, and A. Kramer, Phys. Rev. B **63**, 174508 (2001).

[6] D. Munzar, C. Bernhard, T. Holden, A. Golnik, J. Humlíek, and M. Cardona, Phys. Rev. B **64**, 24523 (2001).

[7] M.S. Kim, J.H. Choi, and S.I. Lee, Phys. Rev. B **63**, 92507 (2001).

[8] Wonkee Kim and J.P. Carbotte, Phys. Rev. B **63**, 54526 (2001).

[9] W.K. Park and Z.G. Khim, Phys. Rev. B **61**, 1530 (2000).

[10] A. Yurgens, D. Winkler, T. Claeson, T. Murayama, and Y. Ando, Phys. Rev. Lett. **82**, 3148 (1999).

[11] H. Shaked, P. M. Keane, and J. C. Rodriguez, *Crystal Structure of the High Tc Superconducting Copper-Oxides* (Elsevier, Amsterdam, 1994).

[12] D.P. Norton, B.C. Chakoumakos, J.D. Budai, D.H. Lowndes, B.C. Sales, J.R. Thompson, and D.K. Christen, Science **265**, 2074 (1994).

[13] M. Kanai and T. Kawai, Physica C **235-240**, 174 (1994).

[14] S. Colonna, F. Arciprete, A. Balzarotti, G. Balestrino, P.G. Medaglia, and G. Petrocelli, Physica C **334**, 64 (2000).

[15] G. Balestrino, S. Lavanga, P.G. Medaglia, S. Martellucci, A. Paoletti, G. Pasquini, G. Petrocelli, A. Tebano, A.A. Varlamov, L. Maritato, and M. Salvato, Phys. Rev. B **62**, 9835 (2000).

[16] G. Balestrino, S. Lavanga, P.G. Medaglia, P. Orgiani, A. Paoletti, G. Pasquini, A. Tebano, and A. Tucciarone, Appl. Phys. Lett. **79**, 99 (2001).

[17] G. Balestrino, S. Lavanga, P.G. Medaglia, P. Orgiani, and A. Tebano, Phys. Rev. B **64**, 020506 (2001).

[18] J.M. Triscone, O. Fischer, O. Brunner, L. Antognazza, A.D. Kent, and M.G. Karkut, Phys. Rev. Lett. **64**, 804 (1990).

[19] Z.Z. Li, H. Rifi, A. Vaurès, S. Megtert, and H. Raffy, Phys. Rev. Lett. **72**, 4033 (1994).

[20] J.H. Schön, M. Dorget, F.C. Beuran, X.Z. Zu, E. Arushanov, C. Deville Cavellin, and M. Lagues, Nature (London) **414**, 434 (2001).

[21] G. Balestrino, S. Martellucci, P.G. Medaglia, A. Paoletti, and G. Petrocelli, Physica C **302**, 78 (1997).

[22] A. Tebano, G. Balestrino, S. Lavanga, S. Martellucci, P.G. Medaglia, A. Paoletti, G. Pasquini, G. Petrocelli, and A. Tucciarone, Physica C **355**, 335 (2001).

[23] E.E. Fullerton, J. Guimpel, O. Nakamura, and I.K. Schuller, Phys. Rev. Lett. **69**, 2859 (1992).

[24] M. Varela, W. Grogger, D. Arias, Z. Sefriouri, C. Leon, C. Ballesteros, K.M. Krishnan, and J. Santamaria, Phys. Rev. Lett. **86**, 5156 (2001).

[25] E.E. Fullerton, I.K. Schuller, H. Vanderstraeten, and Y. Bruynseraede, Phys. Rev. B **45**, 9292 (1992).

[26] D.B. Haviland, Y. Liu, and A.M. Goldman, Phys. Rev. Lett. **62**, 2180 (1989).

[27] U. Kabasawa, T. Fukazawa, H. Hasegawa, Y. Tarutani, and K. Takagi, Phys. Rev. B **55**, 716 (1997).